BRAIN CONNECTIVITY
Volume 5, Number 5, 2015

DOI: 10.1089/brain.2014.0308

Disrupted Brain Functional Organization in Epilepsy Revealed by Graph Theory Analysis

Jie Song,[1,2] Veena A. Nair,[2] Wolfgang Gaggl,[2] and Vivek Prabhakaran[1–7]

Abstract

The human brain is a complex and dynamic system that can be modeled as a large-scale brain network to better understand the reorganizational changes secondary to epilepsy. In this study, we developed a brain functional network model using graph theory methods applied to resting-state fMRI data acquired from a group of epilepsy patients and age- and gender-matched healthy controls. A brain functional network model was constructed based on resting-state functional connectivity. A minimum spanning tree combined with proportional thresholding approach was used to obtain sparse connectivity matrices for each subject, which formed the basis of brain networks. We examined the brain reorganizational changes in epilepsy thoroughly at the level of the whole brain, the functional network, and individual brain regions. At the whole-brain level, local efficiency was significantly decreased in epilepsy patients compared with the healthy controls. However, global efficiency was significantly increased in epilepsy due to increased number of functional connections between networks (although weakly connected). At the functional network level, there were significant proportions of newly formed connections between the default mode network and other networks and between the subcortical network and other networks. There was a significant proportion of decreasing connections between the cingulo-opercular task control network and other networks. Individual brain regions from different functional networks, however, showed a distinct pattern of reorganizational changes in epilepsy. These findings suggest that epilepsy alters brain efficiency in a consistent pattern at the whole-brain level, yet alters brain functional networks and individual brain regions differently.

Key words: epilepsy; functional networks; graph theory; network analysis

Introduction

The human brain can be modeled as a network or a graph represented by a collection of nodes (i.e., cortical and subcortical brain regions) and links (i.e., associations between nodes) (Sporns et al., 2005). This approach is based on graph theory, which provides a powerful way of examining the dynamic interactions among multiple brain regions and how these interactions produce complex behaviors in human beings. This approach has provided insights into many neurological disorders, including epilepsy, and has the potential to provide useful biomarkers for diagnostic and prognostic purposes (Haneef and Chiang, 2014). By definition, an epileptic seizure is a transient occurrence of signs and/or symptoms due to abnormal, excessive, or synchronous neuronal activity in the brain (Fisher et al., 2005). This regional, abnormal neuronal activity could potentially disrupt the base connectivity of individual brain regions as well as brain networks. Previous studies on epilepsy have shown topological changes of whole-brain functional networks in temporal lobe epilepsy (TLE) (Doucet et al., 2015; Wang et al., 2014) and in idiopathic generalized epilepsy (IGE) (Zhang et al., 2011). These studies showed epilepsy-related impairments in the whole-brain functional networks, including reduced clustering coefficient and increased global efficiency in TLE and IGE patients relative to healthy controls.

In the current study, we developed a network model based on resting-state functional connectivity (RSFC) using graph theory to examine the epileptic reorganizational changes in brain functional networks at the whole-brain level and regional level. Higher-order graph-theoretic measures such as local efficiency and global efficiency along with lower-order measures such as strength and degree are estimated to quantify brain network organization and to compare epileptic

Departments of [1]Biomedical Engineering and [2]Radiology, University of Wisconsin-Madison, Madison, Wisconsin.
[3]Neuroscience Training Program and [4]Medical Scientist Training Program, University of Wisconsin-Madison, Madison, Wisconsin.
Departments of [5]Neurology, [6]Psychiatry, and [7]Psychology, University of Wisconsin-Madison, Madison, Wisconsin.

brains with age- and gender-matched healthy controls. We hypothesize that the local efficiency and global efficiency can be affected by epilepsy and that epileptic disruptions may display a distinct pattern across brain regions and networks. In this study, we examined brain functional network reorganization at the whole-brain level, individual functional networks, and individual brain regions to better understand the underlying mechanism of these reorganizational changes.

Methods

Subjects

Current findings are based on data acquired from nine epilepsy patients (33.8 ± 9.4 years, 6 F/3 M) and nine age- and gender-matched healthy control subjects (33 ± 10.4 years, 6 F/3 M) (Supplementary Table S1; Supplementary Data are available online at www.liebertpub.com/brain). No significant ($p < 0.05$) age (two-sample *t*-test, two-tailed, *p*-value = 0.87) or gender differences were found between the two groups. This study was approved by the University of Wisconsin-Madison's Institutional Review Board. All subjects provided written informed consent. Subject profiles are shown in Supplementary Table S1.

Neuroimaging data acquisition

Each epilepsy patient received a 5-min resting-state fMRI scan as part of the clinical examination on a 3.0 Tesla whole-body MRI scanner (DISCOVERY MR750, General Electric Medical Systems, Waukesha, WI) with an 8-channel head coil. MR imaging parameters were single-shot Echo Planar Imaging (EPI), axial plane, TR = 2000 ms, TE = 30 ms, flip angle = 75°, slice thickness = 5 mm, number of slices = 28, acquisition matrix = 64×64, field of view (FOV) = 240×240 mm^2, voxel size = $3.75 \times 3.75 \times 5$ mm^3, and single average (NEX = 1). T1-weighted structural images were acquired axially (TR = 8.688 ms, TE = 3.468 ms, TI = 450 ms, flip angle = 12°, FOV = 240×240 mm^2, voxel size = $0.94 \times 0.94 \times 1.2$ mm^3, number of slices = 136).

Each age- and gender-matched healthy control subject received a 10-min resting-state fMRI scan on the same scanner (only the first 5 min were used for analyses). MR imaging parameters were single-shot EPI, sagittal plane, TR = 2600 ms, TE = 22 ms, flip angle = 60°, slice thickness = 3.5 mm, number of slices = 40, acquisition matrix = 64×64, FOV = 224×224 mm^2, voxel size = $3.5 \times 3.5 \times 3.5$ mm^3, and NEX = 1. T1-weighted structural images with 1-mm isotropic voxels were acquired axially (TR = 8.132 ms, TE = 3.18 ms, TI = 450 ms, flip angle = 12°, FOV = 256×256 mm^2, number of slices = 156).

Imaging data preprocessing

Resting-state fMRI data was processed in AFNI (Cox, 1996) following the recommended processing pipeline (Jo et al., 2013) for controlling head motion. The preprocessing steps included (1) despiking to remove extreme outliers in the signal intensity time courses, (2) correcting for motion and slice timing, and (3) removing the first three time points of the scan. T1-weighted structural images were warped to standard MNI space using a 12-parameter affine transformation. This transformation was combined with T1-to-EPI alignment and used to map the functional EPI scans to MNI space with a resampling of 3 mm resolution. The resulting structural images were later skull stripped and segmented into gray matter, white matter (WM), and cerebrospinal fluid (CSF) masks using FSL (Smith et al. 2004). The average signal time course from the WM and CSF masks and the six rigid body motion parameters were normalized and regressed out. The residuals from the functional data were spatially smoothed with a 4×4 mm^2 full-width half-maximum isotropic Gaussian kernel in AFNI, and then temporally filtered with a band pass from 0.01 to 0.1 Hz.

Head motion has been shown to significantly affect the RSFC measures (Saad et al., 2009; Satterthwaite et al., 2012; Van Dijk et al., 2012). In the current study, a secondary motion correction was performed to exclude fMRI volumes (i.e., time frames/points) with motion above a threshold. A score of motion measurement corresponding to each volume was calculated as the square root of the sum of squares of the derivatives (SSD) of the six time courses of the motion parameters (Birn et al., 2013; Jones et al., 2010; Meier et al., 2012). A stringent threshold of SSD was set at 0.2 mm; in other words, any time frame associated with a score of SSD greater than 0.2 mm was censored and later excluded using the censor option provided in the AFNI program, 3dDeconvolve. This option essentially performed zero filling to maintain the same sampling rate for each subject. Head motion evaluated with the average SSD scores per subject showed no significant group difference between epilepsy patients (0.056 ± 0.021 mm) and healthy controls (0.048 ± 0.015 mm) after correcting for motion (two-sample *t*-test, two-tailed, *p*-value = 0.36).

To avoid the potentially confounding effect of the different rs-fMRI scan lengths (i.e., 5 min for epilepsy patients, but 10 min for healthy controls), we only used the first 5 min from each age- and gender-matched healthy control subject.

Brain network construction

Brain networks were constructed based on RSFC. A total of 187 brain regions of interest (ROIs) (Supplementary Fig. S1) were predefined within the sensorimotor, cingulo-opercular task control, frontoparietal task control, dorsal/ventral attention, default mode, salience, and subcortical/cerebellar networks (Power et al., 2011). An averaged time series signal resulting from the preprocessed rs-fMRI data was extracted from each of these 187 regions with a radius of 4 mm. Pearson's correlation coefficient (r_{ij}) was calculated for the *i*th and *j*th ROI. This process generated a 187×187 connectivity matrix for each subject within each group. We then thresholded each of these connectivity matrices using a minimum spanning tree (MST) approach to obtain a sparse connectivity matrix with optimal functional connections for detecting epileptic alterations of the brain networks (Song et al., 2014). Each MST per subject is a spanning tree of a weighted subgraph that is fully connected with all nodes containing maximum total weights of all links, which can be considered as the skeleton structure of the brain network for each subject. However, these MSTs do not form clusters or loops among individual brain regions, which keep it from a biologically meaningful sparse representation of brain networks (Alexander-Bloch et al., 2010). To obtain a sparse yet biologically meaningful connectivity matrix, proportions of

the remaining connections were added to the MST to form clusters or loops among brain regions. To do so, the top 2%, 4%, 6%, and 8% of the remaining connections from the MST-extracted connectivity matrix were added to the MST, respectively. This resulted in four sparse connectivity matrices with four levels of highest proportion of functional connections from the original connectivity matrix for each subject. This approach ensured that (1) each sparse connectivity matrix for each epilepsy patient and healthy control subject contained an equal number of functional connections and that (2) a range of different proportional thresholds was examined to access the effect of thresholding on group comparisons.

Network analysis

Graph-theoretic analyses were applied to the sparse connectivity matrices. Graph metrics, including local efficiency, global efficiency, and strength, were estimated using the Brain Connectivity Toolbox (Rubinov and Sporns, 2010). The Brain Connectivity Toolbox provided calculations of these metrics at the whole-brain level across all regions. In the current study, we made adaptation to the original scripts to calculate these metrics for individual brain regions. The epilepsy patients and control subjects were compared across 187 brain regions with each graph-theoretic measure estimated for each brain region and averaged across subjects within each group.

Local efficiency is a measure of information transmission among locally connected regions, such as in a module or a subnetwork, whereas global efficiency is a measure of system-wide (i.e., over the whole brain) information transmission. Local efficiency quantifies the extent that connections are being segregated into local clusters or subnetworks (Achard et al., 2012), whereas global efficiency quantifies the extent that connections are being integrated into a system-wide network (Rubinov and Sporns, 2010). These two higher-level graph metrics were estimated on unweighted graphs (Achard et al., 2012). Strength and degree are two lower-level graph metrics that measure how strongly connections are formed over the whole brain or at individual brain regions. Strength is estimated as the mean value of weights (i.e., Pearson's cross-correlation coefficients) of all functional connections linking to a particular brain region or across multiple brain regions and is measured on weighted graphs. It is worth pointing out that the use of negative connections (such as functional anticorrelations with negative correlation coefficients) in graph-theory-based connectivity studies remains highly debated (Achard and Bullmore, 2009; Fair et al., 2009; Rubinov and Sporns, 2010) and may tend to decrease test-retest reliability of global network properties (Wang et al., 2011). In the current study, all self-connections or negative connections were removed from the networks before analysis. The degree, an unweighted measure of functional connections, is estimated as the number of functional connections linking to a particular brain region that survived thresholding on unweighted graphs.

Estimating brain network disruptions in epilepsy

Epilepsy may disrupt brain network organization differently across regional locations and functional networks. We adopted a similar approach that was originally used for detecting functional network changes in comatose patients and referred to as the hub disruption index, κ (Achard et al., 2012). The hub disruption index for a given graph metric, for example, strength, was constructed by subtracting the mean regional strength of the healthy control group from the mean strength of the corresponding brain region in the epilepsy group and plotting this group mean difference against the healthy control group mean. The slope of a straight line fitted to the data was referred to as hub disruption index, κ. This approach essentially provided a visualization as well as estimation for examining network and brain regional disruptions combined from a single plot.

Statistical analysis

Group comparison was conducted for each graph metric at each threshold level using nonparametric Wilcoxon rank sum test (one-sided) to avoid invalid assumption of Gaussian distribution of these metric values in each group. As group comparisons were conducted at each threshold of connection density (i.e., top 2%, 4%, 6%, and 8%), an adjusted Bonferroni method was applied to correct for multiple comparisons (Holm, 1979). One-sided binomial proportion tests were later used to compare the proportions of strength and degree of each network to the total strength and degree of whole-brain networks, respectively, between the two groups (Song et al., 2012). The same Bonferroni method was applied to correct for multiple comparisons made at different networks (i.e., sensorimotor network, default mode network [DMN], cingulo-opercular network, etc). All statistical tests were evaluated at a significance level of 0.05.

Results

Disrupted local efficiency in epilepsy

At the whole-brain level, we found that local efficiency was significantly decreased in epilepsy across a range of thresholds (Fig. 1). Group mean local efficiency increased

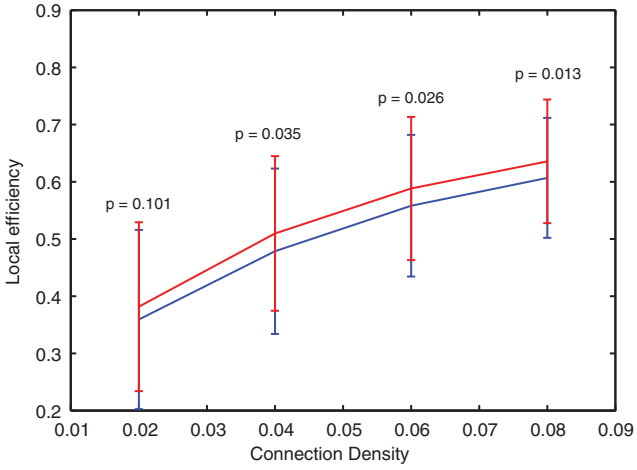

FIG. 1. Local efficiency compared between epilepsy and healthy control subjects. The epilepsy patients show significantly decreased local efficiency across a range of thresholds/connection densities (p-values listed are corrected for multiple comparisons, Wilcoxon rank sum tests.) (Epilepsy-blue line, Healthy control-red line).

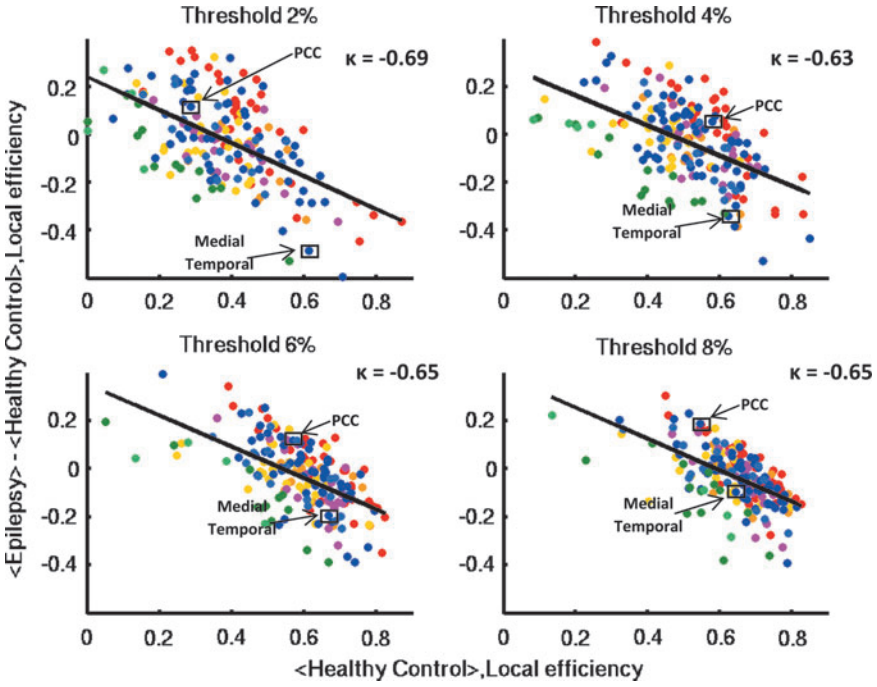

FIG. 2. Hub disruption index of local efficiency. The hub disruption index of local efficiency is plotted at each threshold of connection density. Each data point is color coded representing a node belonging to a particular functional network (i.e., red dots represent nodes belonging to the sensorimotor network, and blue dots represent nodes belonging to the DMN). The mean value of local efficiency of each node in the healthy control group <Healthy Control> (x-axis) is plotted against the difference between groups in mean local efficiency of each node <Epilepsy> - <Healthy Control> (y-axis). The hub disruption index of local efficiency is then estimated as the slope of the solid black line fitted to the scatter plots. Negative hub disruption indices are observed across different thresholds, indicating an overall disruption of local efficiency in the epilepsy group. Compared with the healthy control group, the epilepsy patients show a distinct pattern of regional changes in local efficiency. The posterior cingulate cortex (PCC) has increased local efficiency, whereas the medial temporal lobe shows decreased local efficiency.

monotonically as a function of increasing connection density. Local efficiency decreased in regions such as the medial temporal lobe of the DMN and postcentral gyrus (PCG) of the sensorimotor network. However, increased local efficiency was observed in some regions, such as the posterior cingulate cortex (PCC) and angular gyrus from the DMN, thalamus from the subcortical network, and cerebellar vermis from the cerebellar network. A negative hub disruption index ($\kappa < -0.6$) was observed across all thresholds (Fig. 2). In other words, brain regions with high information processing efficiency in healthy control subjects showed great reduction in epilepsy patients (i.e., medial temporal lobe), whereas brain regions with normal information processing efficiency in healthy controls showed abnormal increase in patients (i.e., PCC).

Disrupted global efficiency in epilepsy

At the whole-brain level, global efficiency was significantly increased in epilepsy across a range of thresholds (Fig. 3). Group mean global efficiency increased monotonically as a function of increasing connection density. A negative hub disruption index of global efficiency ($\kappa < -0.4$) was observed across all thresholds (Supplementary Fig. S2). Similar to what was found in local efficiency, a distinct pattern of changes in global efficiency across different brain regions was observed. The medial temporal lobe and PCG continued to show decreased global efficiency, whereas the PCC, angular gyrus, thalamus, and cerebellar vermis continued to show increased global efficiency.

Increased yet weakly connected between-network functional connections

At the whole-brain level, both groups had similar functional connection strength that increased monotonically as a function of increasing connection density (Fig. 4). A negative hub disruption index of functional strength ($\kappa < -0.4$) was observed across all thresholds (Supplementary Fig. S3).

To further examine the reorganizational changes for each functional network, we conducted a second-level analysis based on two basic graph metrics—strength and degree. We found that within each functional network, there was no significant difference between the two groups in terms of the number or strength of connections (binomial proportional tests, p-value > 0.05; Supplementary Fig. S4). However, there was an increased number of between-network connections in the epilepsy patients (Fig. 5). Three functional networks showed significant group differences (Table 1). Epilepsy patients had a significantly decreased proportion of between-network connections in the cingulo-opercular task control network (binomial proportional tests,

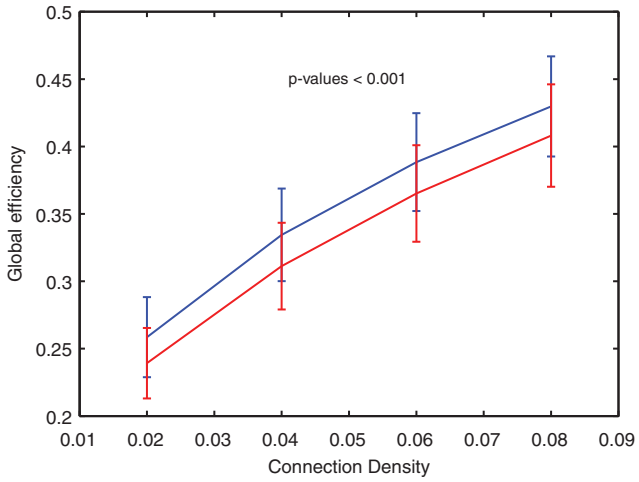

FIG. 3. Global efficiency compared between epilepsy and healthy control subjects. Global efficiency is significantly increased in the epilepsy group across a range of different connection densities (Wilcoxon rank sum tests, p-values <0.001 with multiple comparison correction) (Epilepsy-blue line, Healthy control-red line).

corrected p-value <0.001) and a significantly increased proportion of between-network connections in the DMN and subcortical network (binomial proportional tests, corrected p-values <0.001). However, the corresponding functional strength of these newly formed between-network connections was not significantly different between the two groups (Supplementary Table S2), suggesting that these connections were weakly connected.

Discussion

Previous studies have examined brain efficiency in both functional networks (Vlooswijk et al., 2011; Wang et al., 2014; Zhang et al., 2011) and structural networks in epilepsy (Bernhardt et al., 2011; Liu et al., 2014). However, these findings have remained conflicting potentially due to various factors such as different data processing approach and heterogeneous study population. In the present study, we matched each epilepsy patient with an age- and gender-matched healthy control subject and have taken stringent steps to safeguard against head motion artifact following the recommended data processing pipeline (Jo et al., 2013). Furthermore, graph theory metrics were assessed at the regional level for each ROI following consideration of different thresholds upon network calculations. Besides these traditional graph metrics, a hub disruption index was calculated for these metrics to better visualize the epileptic disruptions across different networks and brain regions. Only a small number of patients were included into the current study, which might

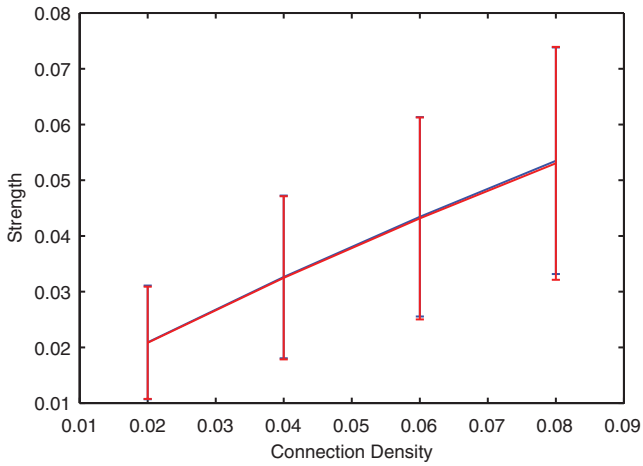

FIG. 4. Connection strength compared between epilepsy and healthy control subjects. Functional connection strength is statistically similar between the epilepsy and healthy control groups across a range of different connection densities (Wilcoxon rank sum tests, p-values >0.05) (Epilepsy-blue line, Healthy control-red line).

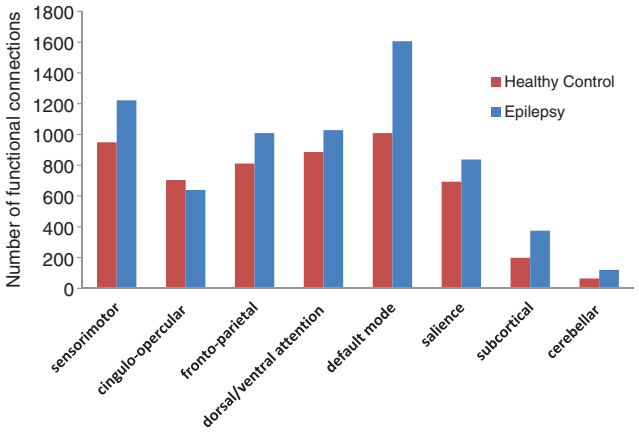

FIG. 5. Between-network functional connections in epilepsy. Overall, there is an increased number of functional connections between networks in the epilepsy patients.

TABLE 1. DEGREE OF FUNCTIONAL CONNECTIONS BETWEEN NETWORKS

Functional network	*Proportion of degree of between-network connections*			
	Healthy Control	*Epilepsy*	*Corrected* p-*value*	*Directional change*
Sensorimotor	0.179	0.179		
Cingulo-opercular	**0.132**	**0.093**	**<0.001**	⬇
Frontoparietal	0.153	0.148		
Dorsal/ventral attention	0.167	0.150	0.06	
Default mode	**0.190**	**0.235**	**<0.001**	⬆
Salience	0.130	0.122		
Subcortical	**0.037**	**0.055**	**<0.001**	⬆
Cerebellar	0.012	0.018	0.07	

Binomial proportional test was used to compare the proportion of between-network connections for each functional network, followed by multiple comparison correction. The cingulo-opercular network showed significantly decreased between-network connections (p-value <0.001), whereas the default mode and subcortical network showed significantly increased between-network connections (p-value <0.001).

limit the power, but can also be regarded as strength, as we still showed a significant difference between epilepsy patients and healthy control subjects.

Disrupted network efficiency

We observed a whole-brain disruption of both local efficiency and global efficiency in epilepsy patients, consistent with previous studies (Doucet et al., 2015; Vlooswijk et al., 2011). Local efficiency was significantly decreased in patients with epilepsy (Fig. 1), suggesting impaired regional information transmission and a disruption of network segregation (Rubinov and Sporns, 2010). In contrast, global efficiency was significantly increased in epilepsy (Fig. 3), suggesting a higher efficiency for global information transmission, which may be a marker of abnormal transmission such as seizure propagation (Rubinov and Sporns, 2010). Both local efficiency and global efficiency tend to decline with a negative hub disruption index compared with healthy controls when examined at the functional network level (Fig 2 and Supplementary Fig. S1), indicating an exchange of higher efficiency regions to lower efficiency regions. In addition, these regional reorganizations reveal an alteration of functional importance of individual regions within the same functional network due to epilepsy, which may not be easily observed from a brain-wide network analysis.

We observed that the medial temporal lobe from the DMN and PCG from the sensorimotor network consistently showed decreased efficiency, whereas the PCC and angular gyrus from the DMN, thalamus from the subcortical network, and cerebellar vermis from the cerebellar network showed increased efficiency. These regions are critical areas in corresponding functional networks. We conducted secondary network analyses for each functional network to further examine if these changes are adaptive or maladaptive.

Abnormally increased weak connections between networks

A finer-grained network analysis was performed to examine the changes in the number and strength of connections within and between networks. Besides similar whole-brain functional strength (Fig. 4), there were no significant differences in terms of the number or strength of connections within each functional network between the two groups (Supplementary Fig. S4). However, there was a markedly increased number of between-network connections (Supplementary Fig. S5) in the epilepsy group. Further statistical analysis demonstrated that the DMN and subcortical networks had a significantly increased number of connections to all other networks (Table 1). There was also a small yet significant amount of connections that decreased between the cingulo-opercular network and other networks. Overall, there was an increase in between-network connections in the epilepsy group. Nevertheless, these newly formed connections between networks were shown to be weakly connected as the functional strength of between-network connections was not significantly different between the epilepsy and healthy control subjects (Supplementary Table S2). This finding further supports the observation of increased global efficiency, which is potentially elevated by the increased amount of shortest path length for long-distance information processing (Rubinov and Sporns, 2010).

Limitations

The small sample size ($n = 9$) and the heterogeneity of seizure location and duration were the primary limitations of this study.

First, we used a convenient sample comprising previously collected data without prior coordination of acquisition parameters such as different echo time, repetition time, and voxel size. Although a previous study showed that failure to hold these acquisition parameters constant might lead to systematic differences when studied in the context of multicenter fMRI studies (Glover et al., 2012), one of our previous studies showed a high level of reliability of RSFC in normal healthy subjects with different acquisition parameters (Song et al., 2012). Further interpretations based on findings reported here should proceed with caution.

Second, it was reported that the presence of head motion tends to bias the correlations (Saad et al., 2009; Satterthwaite et al., 2012; Van Dijk et al., 2012). Taking these factors into account, in the present study, we had nine epilepsy patients with minimal head motion and matched these patients with control subjects with no significant differences in terms of age, gender, and head motion (described in *Imaging data preprocessing* section). We also ensure that these patients and the control subjects had fMRI data of the same time length. To further test our method in a relatively larger sample, we added another 4 epilepsy patients and 4 age-, gender-, and motion-matched control subjects to the study group and applied the same method and analyses on 13 epilepsy patients versus 13 control subjects (Supplemental Data). These patients and their matched control subjects had the same number of time points of fMRI data after correction for motion, but with variation in terms of the time length of fMRI data. We performed analyses on these 13 patients and 13 control subjects and observed similar findings. This further suggests the robustness of this method based on graph-theoretic measures made at the regional or nodal level. Essentially, we compared the two groups across 187 brain regions with each graph-theoretic measure estimated for each brain region and averaged within the group.

In addition, seven of nine patients were identified to have TLE, while one patient had a different seizure location, and one patient was idiopathic. There are differences in treatments between these different patients in terms of medications as well as two of our patients were status post focal resection, which could also influence brain reorganization (Supplementary Table S1). A recent study (Doucet et al., 2015) suggests that age of seizure onset has an impact on whole-brain and regional RSFC in TLE patients. It would be important to examine brain functional reorganization in a larger and homogenous subset of epilepsy patients (e.g., TLE or mesial temporal sclerosis patients) and evaluate the potential relationship between graph-theoretic and clinical measures.

Another limitation is the robustness of network estimation depending on the applied parcellation method (ICA and anatomic). For future study, we plan to investigate the robustness of different parcellation methods in terms of network estimation as well as group differences.

Conclusion

In the current study, graph-theoretic analysis was applied to RSFC to examine the brain functional network

reorganization in the presence of epilepsy. It provided direct evidence of large-scale network disruption in epilepsy patients. Compared with healthy control subjects, these patients demonstrated impaired local efficiency and increased global efficiency at the brain-wide level. When examined at the functional network level, these patients showed an increased number of connections between networks that are weakly connected, supporting the observations of abnormally high global efficiency. At the individual brain regional level, however, epilepsy patients exhibited distinct pattern of alterations. Our findings suggest that brain-wide network efficiency is affected in the presence of epilepsy. With a finer-grained network analysis at the network and individual brain regional level, epileptic disruption on functional properties may be better understood.

Acknowledgments

The authors thank all patients and healthy volunteers for their participation. We also thank Joshua Suhonen for his generous help of providing clinical information in a timely manner. This work was supported by NIH grants, RC1MH090912-01, K23NS086852, T32GM008692, UL1TR000427, and T32EB011434, by a Coulter Translational Research Award, an American Heart Association Postdoctoral Fellow Research Award, UW Milwaukee-Madison Intercampus Grants, by funding from the UW Graduate School, and by Grants from the Shapiro Foundation and Foundation of ASNR award.

Author Disclosure Statement

The authors have no conflicts of interest to report as this research was conducted in the absence of commercial and financial relationships that might compromise the integrity of the results reported herein.

References

Achard S, Bullmore E. 2009. Efficiency and cost of economical brain functional networks. PLoS Comput Biol 3:e17.

Achard S, Delon-Martin C, Vertes PE, Renard F, Schenck M, Schneider F, Heinrich C, Kremer S, Bullmore ET. 2012. Hubs of brain functional networks are radically reorganized in comatose patients. Proc Natl Acad Sci U S A 109: 20608–20613.

Alexander-Bloch AF, Gogtay N, Meunier D, Birn R, Clasen L, Lalonde F, Lenroot R, Giedd J, Bullmore ET. 2010. Disrupted modularity and local connectivity of brain functional networks in childhood-onset schizophrenia. Front Syst Neurosci 4:147.

Bernhardt BC, Chen Z, He Y, Evans AC, Bernasconi N. 2011. Graph-theoretical analysis reveals disrupted small-world organization of cortical thickness correlation networks in temporal lobe epilepsy. Cereb Cortex 21:2147–2157.

Birn RM, Molloy EK, Patriat R, Parker T, Meier TB, Kirk GR, Nair VA, Meyerand ME, Prabhakaran V. 2013. The effect of scan length on the reliability of resting-state fMRI connectivity estimates. NeuroImage 83:550–558.

Cox RW. 1996. AFNI: software for analysis and visualization of functional magnetic resonance neuroimages. Comput Biomed Res 29:162–173.

Doucet GE, Sharan A, Pustina D, Skidmore C, Sperling MR, Tracy JI. 2015. Early and late age of seizure onset have a differential impact on brain resting-state organization in temporal lobe epilespy. Brain Topogr 28:113–126.

Fair DA, Cohen AL, Power JD, Dosenbach NU, Church JA, Miezin FM, Schlaggar BL, Petersen SE. 2009. Functional brain networks develop from a ''local to distributed'' organization. PLoS Comput Biol 5:e1000381.

Fisher RS, van Emde Boas W, Blume W, Elger C, Genton P, Lee P, Engel J, Jr. 2005. Epileptic seizures and epilepsy: definitions proposed by the International League Against Epilepsy (ILAE) and the International Bureau for Epilepsy (IBE). Epilepsia 46:470–472.

Glover GH, Mueller BA, Turner JA, van Erp TG, Liu TT, Greve DN, Voyvodic JT, Rasmussen J, Brown GG, Keator DB, Calhoun VD, Lee HJ, Ford JM, Mathalon DH, Diaz M, O'Leary DS, Gadde S, Preda A, Lim KO, Wible CG, Stern HS, Belger A, McCarthy G, Ozyurt B, Potkin SG. 2012. Function biomedical informatics research network recommendations for prospective multicenter functional MRI studies. J Magn Reson Imaging 36:39–54.

Haneef Z, Chiang S. 2014. Clinical correlates of graph theory findings in temporal lobe epilepsy. Seizure 23:809–818.

Holm S. 1979. A simple sequentially rejective multiple test procedure. Scand J Stat 6:65–70.

Jo HJ, Gotts SJ, Reynolds RC, Bandettini PA, Martin A, Cox RW, Saad ZS. 2013. Effective preprocessing procedures virtually eliminate distance-dependent motion artifacts in resting state FMRI. J Appl Math 2013. doi: 10.1155/2013/935154.

Jones TB, Bandettini PA, Kenworthy L, Case LK, Milleville SC, Martin A, Birn RM. 2010. Sources of group differences in functional connectivity: an investigation applied to autism spectrum disorder. NeuroImage 49:401–414.

Liu M, Chen Z, Beaulieu C, Gross DW. 2014. Disrupted anatomic white matter network in left mesial temporal lobe epilepsy. Epilepsia 55:674–682.

Meier TB, Desphande AS, Vergun S, Nair VA, Song J, Biswal BB, Meyerand ME, Birn RM, Prabhakaran V. 2012. Support vector machine classification and characterization of age-related reorganization of functional brain networks. NeuroImage 60:601–613.

Power JD, Cohen AL, Nelson SM, Wig GS, Barnes KA, Church JA, Vogel AC, Laumann TO, Miezin FM, Schlaggar BL, Petersen SE. 2011. Functional network organization of the human brain. Neuron 72:665–678.

Rubinov M, Sporns O. 2010. Complex network measures of brain connectivity: uses and interpretations. NeuroImage 52: 1059–1069.

Saad ZS, Glen DR, Chen G, Beauchamp MS, Desai R, Cox RW. 2009. A new method for improving functional-to-structural MRI alignment using local Pearson correlation. NeuroImage 44:839–848.

Satterthwaite TD, Wolf DH, Loughead J, Ruparel K, Elliott MA, Hakonarson H, Gur RC, Gur RE. 2012. Impact of in-scanner head motion on multiple measures of functional connectivity: relevance for studies of neurodevelopment in youth. NeuroImage 60:623–632.

Smith, SM, Jenkinson M, Woolrich MW, Beckman CF, Behrens TEJ, Johansen-Berg H, Bannister PR, De Luca M, Drobnjak I, Flitney DE, Niazy RK, Saunders J, Vickers J, Zhang YY, De Stefano N, Brady JM, and Matthews PM. 2004. Advances in functional and structural MR image analysis and implementation as FSL. Neuroimage 23:S208–S219.

Song J, Birn RM, Boly M, Meier TB, Nair VA, Meyerand ME, Prabhakaran V. 2014. Age-related reorganizational changes in modularity and functional connectivity of human brain networks. Brain Connec 4:662–676.

Song J, Desphande AS, Meier TB, Tudorascu DL, Vergun S, Nair VA, Biswal BB, Meyerand ME, Birn RM, Bellec P, Prabhakaran V. 2012. Age-related differences in test-retest reliability in resting-state brain functional connectivity. PLoS One 7:e49847.

Sporns O, Tononi G, Kotter R. 2005. The human connectome: a structural description of the human brain. PLoS Comput Biol 1:245–251.

Van Dijk KRA, Sabuncu MR, Buckner RL. 2012. The influence of head motion on intrinsic functional connectivity MRI. NeuroImage 59:431–438.

Vlooswijk MC, Vaessen MJ, Jansen JF, de Krom MC, Majoie HJ, Hofman PA, Aldenkamp AP, Backes WH. 2011. Loss of network efficiency associated with cognitive decline in chronic epilepsy. Neurology 77:938–944.

Wang J, Qiu S, Xu Y, Liu Z, Wen X, Hu X, Zhang R, Li M, Wang W, Huang R. 2014. Graph theoretical analysis reveals disrupted topological properties of whole brain functional networks in temporal lobe epilepsy. Clin Neurophysiol 125: 1744–1756.

Wang JH, Zuo XN, Gohel S, Milham MP, Biswal BB, He Y. 2011. Graph theoretical analysis of functional brain networks: test-retest evaluation on short- and long-term resting-state functional MRI data. PLoS One 6:e21976.

Zhang Z, Liao W, Chen H, Mantini D, Ding JR, Xu Q, Wang Z, Yuan C, Chen G, Jiao Q, Lu G. 2011. Altered functional-structural coupling of large-scale brain networks in idiopathic generalized epilepsy. Brain 134:2912–2928.

Address correspondence to:
Jie Song
Wisconsin Institutes for Medical Research
1111 Highland Avenue
Madison, WI, 53705

E-mail: jsong46@wisc.edu

Vivek Prabhakaran
Department of Radiology
University of Wisconsin-Madison
600 Highland Avenue
Madison, WI, 53711

E-mail: vprabhakaran@uwhealth.org